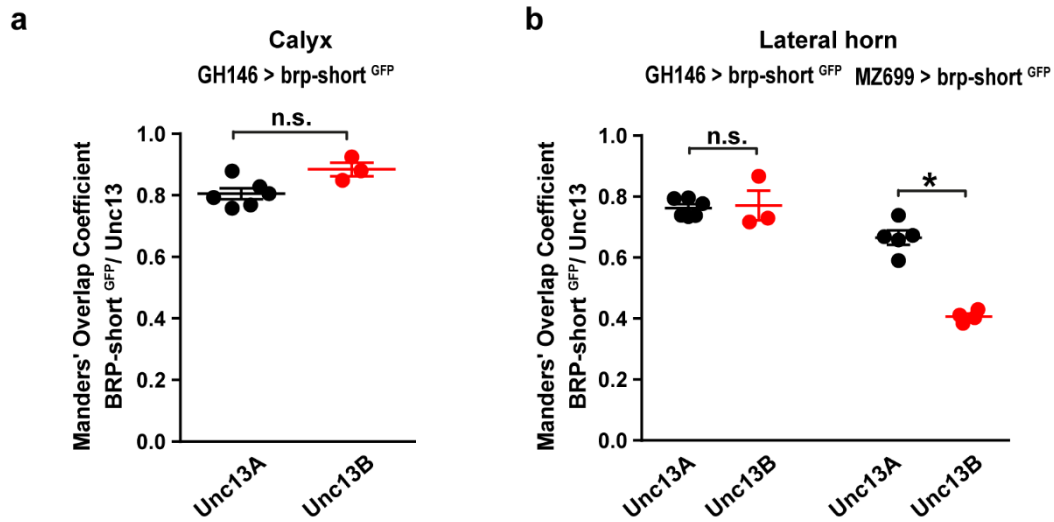


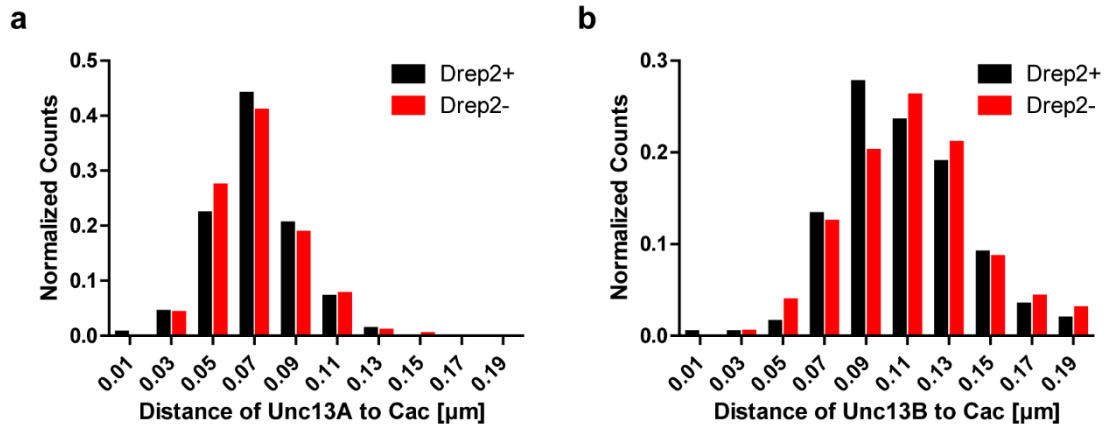
**Unc13A and Unc13B contribute to the decoding of distinct sensory information
in *Drosophila***

Atefeh Pooryasin, Marta Maglione, Marco Schubert, Tanja Matkovic-Rachid, Sayed-mohammad Hasheminasab, Ulrike Pech, André Fiala, Thorsten Mielke, Stephan J. Sigrist

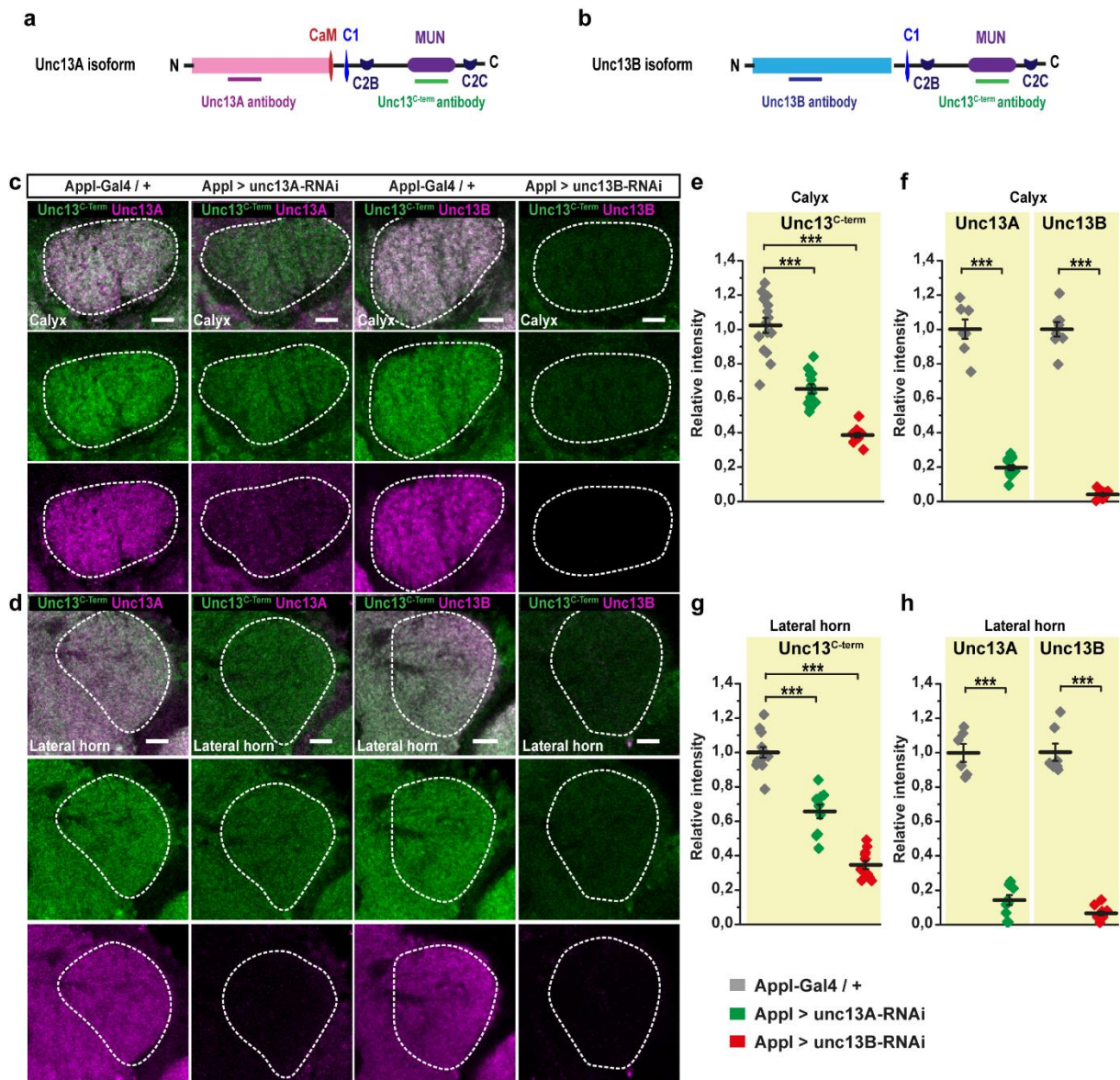
Supplementary Information



Supplementary Figure 1. Unc13A and Unc13B localization relative to BRP-short^{GFP} at active zones of ePNs and iPNs pre-synapses in MB calyx and lateral horn. **a** Mander's overlap coefficient for BRP-short^{GFP} with Unc13A (black) or Unc13B (red) in the MB calyx in flies expressing UAS: brp-short^{GFP} in ePNs (n=3-6). **b** Mander's overlap coefficient for BRP-short^{GFP} with Unc13A (black) or Unc13B (red) in the lateral horn region in flies expressing UAS: brp-short^{GFP} under control of GH146-Gal4 (ePNs, n=3-6) or Mz699-Gal4 (iPNs, n=4-5). Values represent mean \pm SEM. All p-values were calculated via two-tailed Mann-Whitney U test. n.s., not significant ($p > 0.05$), * $p \leq 0.05$. Source data including the exact sample sizes and the p values are provided as a Source Data file.

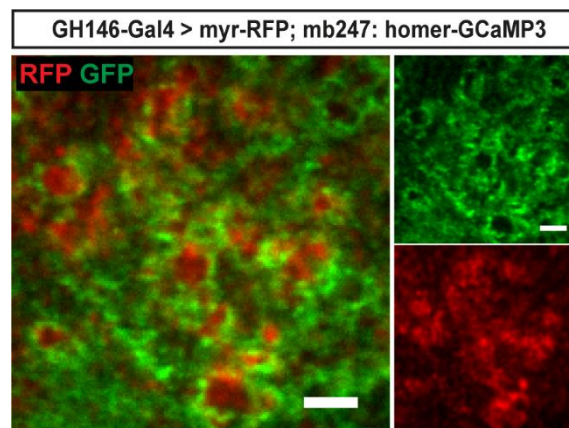


Supplementary Figure 2. Time gated STED analysis of Unc13A and B nano-distribution at LH synapses. **a** Frequency histogram for all Unc13A-sfCac distances found for Drep2-positive (n=323 synapses, 7 brains) and Drep2-negative synapses (n=315 synapses, 7 brains; $p > 0.999$, two samples Kolmogorov-Smirnov test), in the LH. Counts were normalized to obtain a probability density function with an integral equal 1. **b** Frequency histogram for all Unc13B-sfCac distances found for Drep2-positive (n=264 synapses, 7 brains) and Drep2-negative synapses (n=233 synapses, 7 brains; $p = 0.9883$, two samples Kolmogorov-Smirnov test), in the LH. Counts were normalized to obtain a probability density function with an integral equal 1. Source data are provided as a Source Data file.

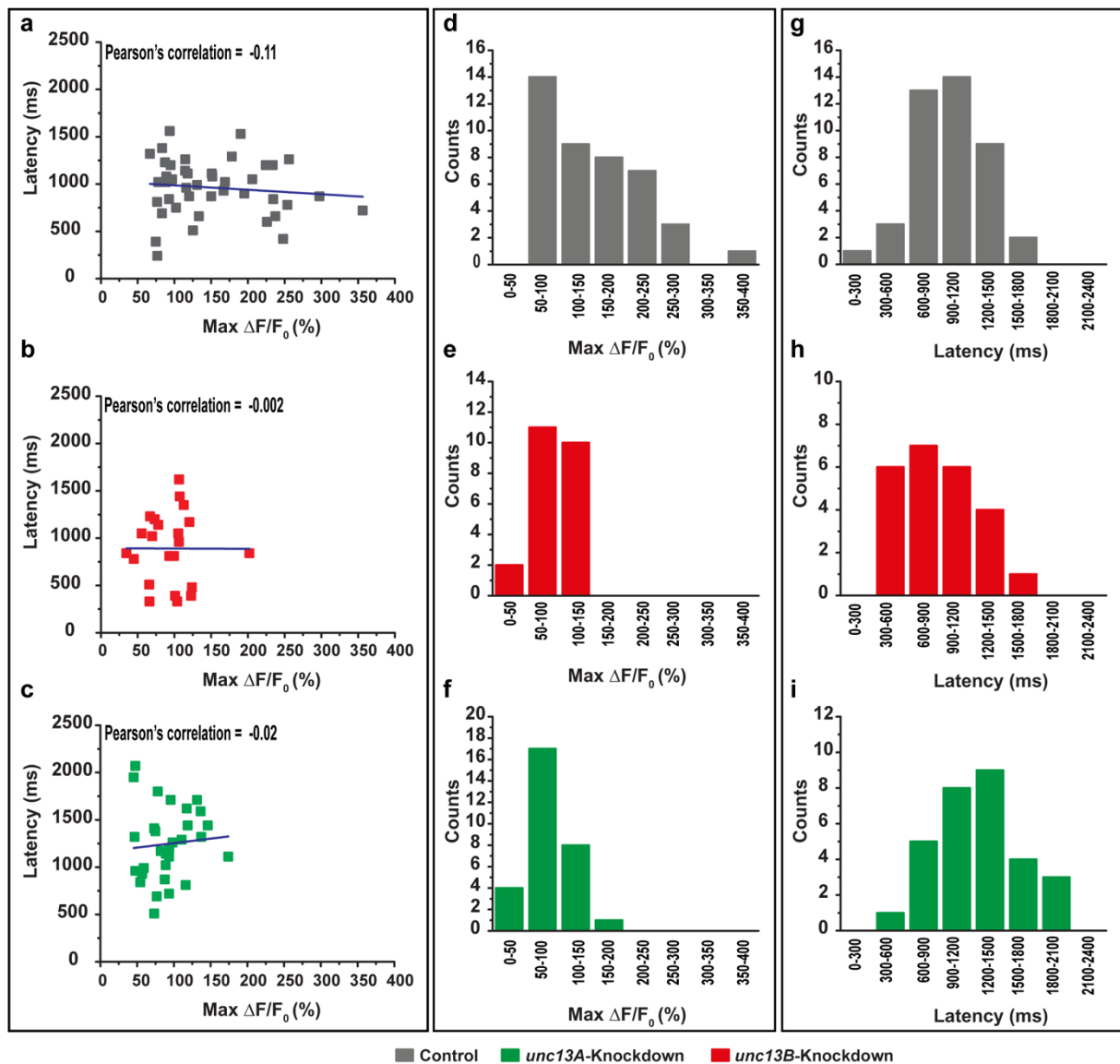


Supplementary Figure 3. Relative levels of Unc13A versus Unc13B in calyx and lateral horn. **a, b** Schematics of Unc13A (**a**) and Unc13B (**b**) constructs indicating CaM, calmodulin; C1, C2B, C2C, and the MUN domain. The Unc13^{C-term} antibody and isoform specific Unc13A and Unc13B antibody epitopes are indicated. **c, d** Confocal images from the calyx (**c**) and lateral horn (**d**) regions in animals expressing UAS: unc13A-RNAi under control of Appl-Gal4, compared to heterozygous driver line, Appl, immunostained against Unc13^{C-term} (green) and Unc13A (magenta) or in animals expressing UAS: unc13B-RNAi under control of Appl-Gal4, compared to heterozygous driver line, Appl, immunostained against Unc13^{C-term} (green) and Unc13B (magenta). Scale bars: 10 μm. **e, g** Expression level of Unc13^{C-term} protein in calyx (**e**) and lateral horn (**g**) regions in animals expressing UAS: unc13A-RNAi or UAS: unc13B-RNAi under control of Appl-Gal4, compared to heterozygous driver line, Appl. The remaining

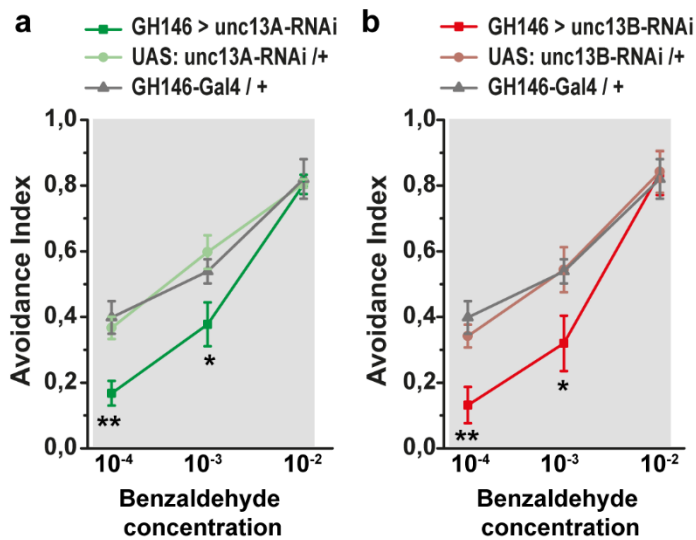
Unc13^{C-term} signal in *unc13A* knockdown animals which represents the Unc13B level in calyx (0.63 ± 0.02) and in lateral horn (0.65 ± 0.03) were measured. The remaining Unc13^{C-term} signal in *unc13B* knockdown animals which represents Unc13A level in calyx (0.36 ± 0.03) and in lateral horn (0.34 ± 0.03) were measured ($n = 10-15$). P-values were calculated via one-way ANOVA with the Bonferroni multiple comparison *post hoc* test ($***p \leq 0.001$). **f, h** Expression level of Unc13A or Unc13B protein in calyx (**f**) and lateral horn (**h**) regions in animals expressing UAS: *unc13A*-RNAi or UAS: *unc13B*-RNAi under control of Appl-Gal4, compared to heterozygous driver line, Appl. The values show a significant reduction of Unc13A in *unc13A* knockdown group (green) compared to the control group (gray plot). The level of Unc13B significantly reduced in *unc13B* knockdown group (red plot) compared to the control group (gray plot) ($n = 6-13$). P-values were calculated via two-sample t-test ($***p \leq 0.001$). Values represent mean \pm SEM. ($***p \leq 0.001$). Source data including the exact sample sizes and the p values are provided as a Source Data file.



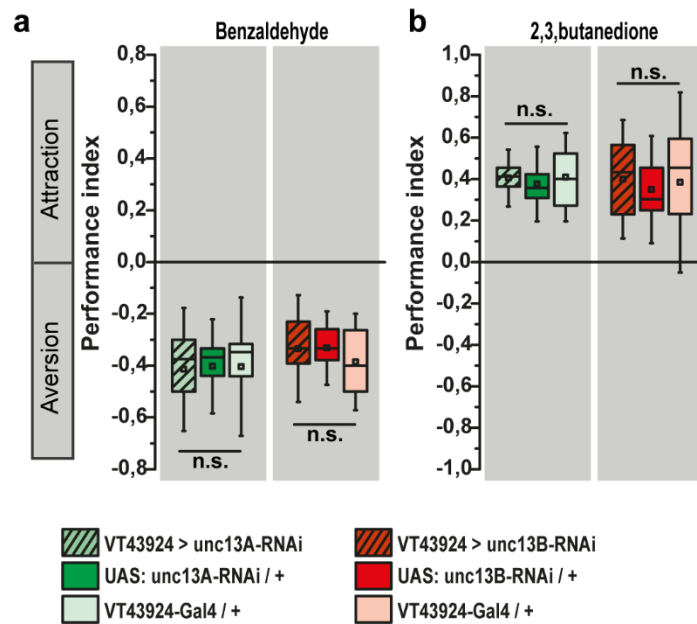
Supplementary Figure 4. Expression pattern of homer-GCaMP3 in the MB Calyx. Visualizing microglomerular structures in the calyx region of animals expressing homer-GCaMP3 sensor in MB postsynaptic terminals under control of mb247 promoter (mb247: homer-GCaMP3) and myr-RFP in ePNs under the control of GH146-Gal4. Green: anti-GFP immunostaining against homer-GCaMP3; Red: anti-RFP immunostaining in presynaptic terminals of ePNs ($n=3$, the experiment was performed once). Scale bars: 2 μ m.



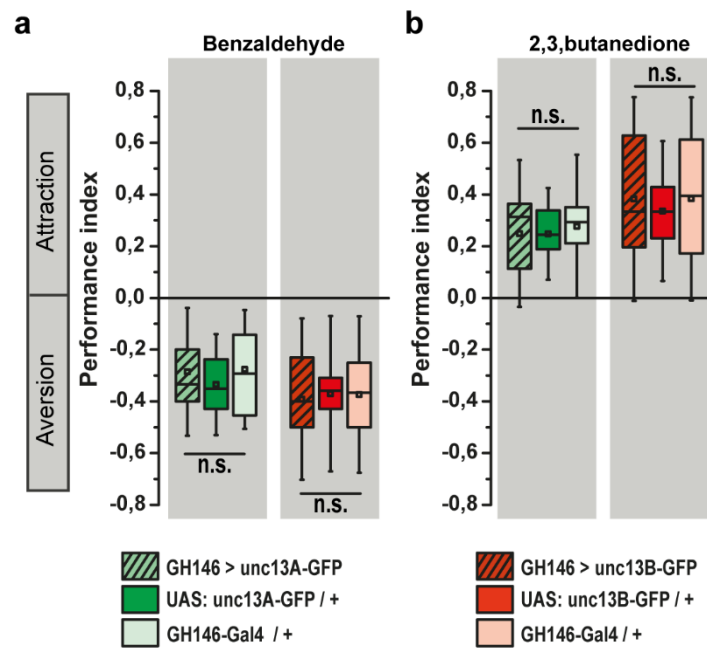
Supplementary Figure 5. Release kinetics (latencies) and Ca^{2+} signal amplitudes across different odor responsive microglomeruli. **a-c** The maximum amplitude ($\Delta F/F_0$) plotted against time to peak (latency) for each responsive microglomerulus for control (*GH146-Gal4/+; mb247: homer-GCaMP3/+*), *unc13B*-knockdown (*GH146 > unc13B-RNAi; mb247: homer-GCaMP3*) and *unc13A*-knockdown (*GH146 > unc13A-RNAi; mb247: homer-GCaMP3*) groups. The Pearson's correlation scores show no correlation between amplitude and the latency in any group. **d-i** Frequency histogram for maximum amplitude ($\Delta F/F_0$) (**d-f**) and time to peak (latency) (**g-i**) for control (*GH146-Gal4/+; mb247: homer-GCaMP3/+*), *unc13B*-knockdown (*GH146 > unc13B-RNAi; mb247: homer-GCaMP3*) and *unc13A*-knockdown (*GH146 > unc13A-RNAi; mb247: homer-GCaMP3*) groups across different odor responsive microglomeruli. Odor stimulation: 4-methylcyclohexanol. n=24-42 microglomeruli, 8-12 animals. Experiment was performed four times. Source data including the exact sample sizes are provided as a Source Data file.



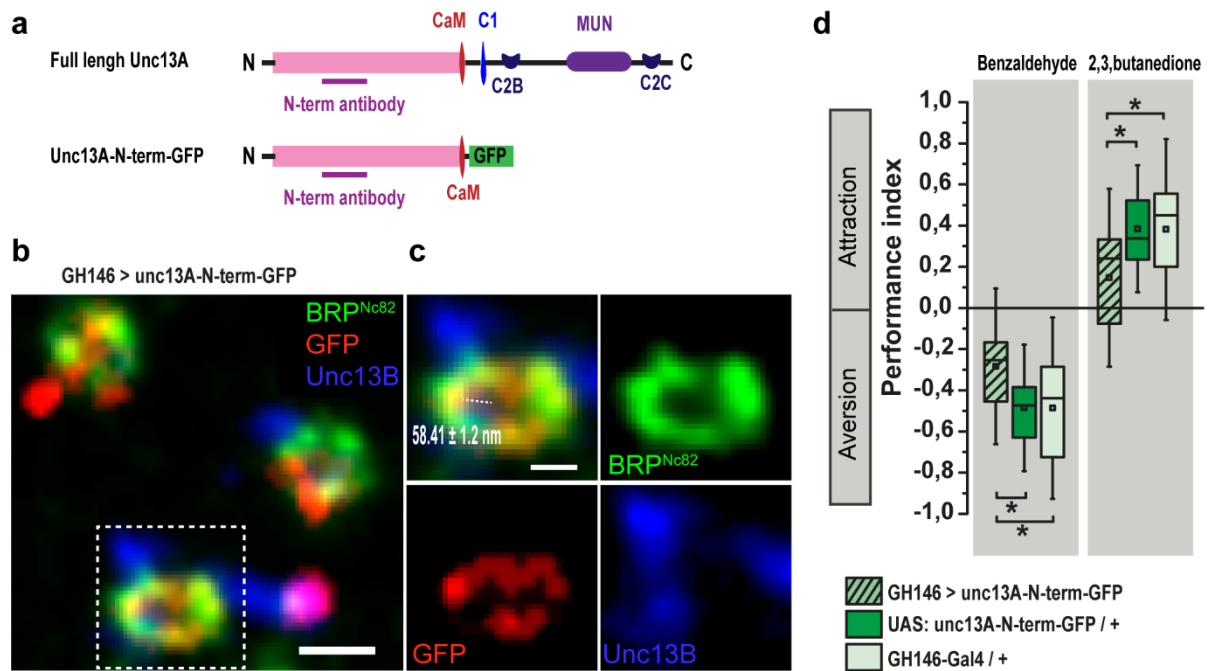
Supplementary Figure 6. Olfactory behavior toward different concentrations of aversive odor after down regulation of *unc13A* or *unc13B* in ePNs Knockdown of *unc13A* (**a**) or *unc13B* (**b**) under control of GH146-Gal4 reduces the performance index of animals toward aversive odor benzaldehyde in low concentrations (diluted 10⁻⁴ and 10⁻³ in paraffin oil, n=9-12). No significant change was observed for high concentration of benzaldehyde (diluted 10⁻² in paraffin oil, n=4-6). All p-values were calculated via one-way ANOVA with the Bonferroni multiple comparison *post hoc* test (*p≤0.05, **p≤0.01). Graphs indicate mean ± SEM. Source data including the exact sample sizes and the p values are provided as a Source Data file



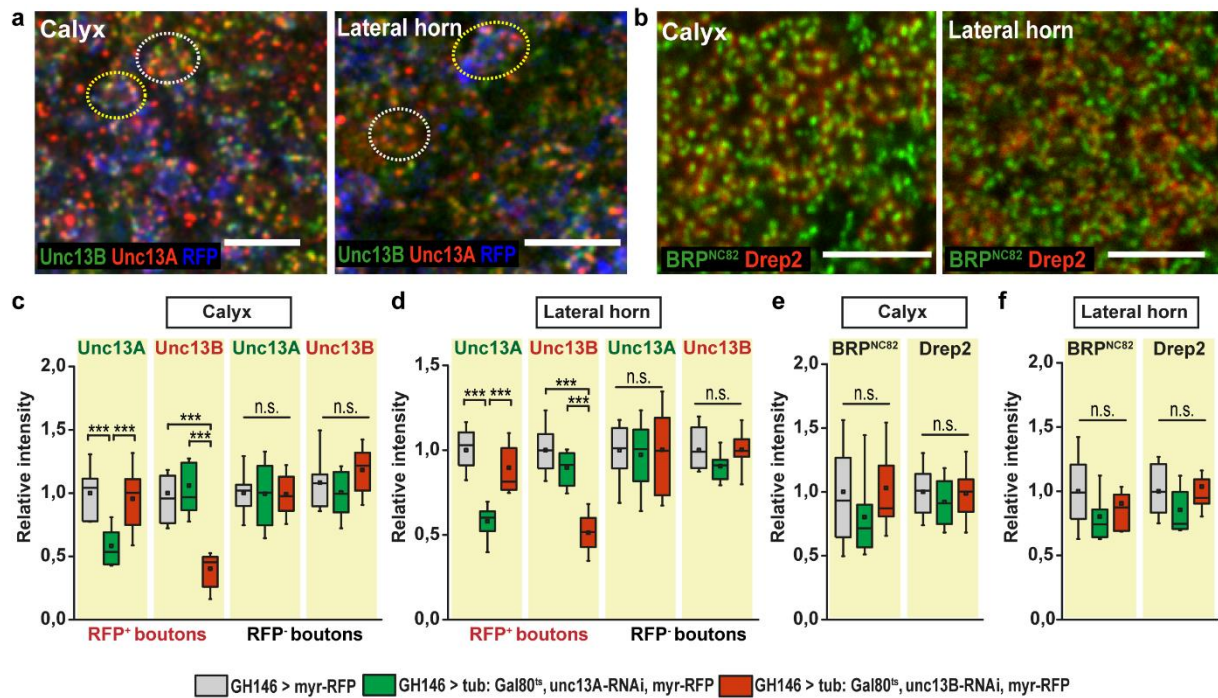
Supplementary Figure 7. Role of APL neurons in olfactory behavior. **a, b.** *unc13A* knockdown or *unc13B* knockdown in APL neurons using VT43924-Gal4 driver line has no significant effect in performance index of animals toward aversive (benzaldehyde n=13-22) and appetitive (2, 3-butanedione, n=14-22) odors. P-values were calculated via one-way ANOVA with the Bonferroni multiple comparison *post hoc* test, n.s., not significant ($p > 0.05$). Box plots indicate means (black squares), medians (middle lines), 25th and 75th percentile ranges (boxes), and SD ranges (whiskers). Source data including the exact sample sizes and the p values are provided as a Source Data file.



Supplementary Figure 8. Overexpression of the *unc13A* or *unc13B* in ePNs. **a, b.** *unc13A-GFP* or *unc13B-GFP* overexpression in ePNs neurons using GH146-Gal4 driver line has no significant effect in performance index of animals toward aversive (benzaldehyde n=14-17) and appetitive (2, 3-butanedione, n=16-19) odors. P-values were calculated via one-way ANOVA with the Bonferroni multiple comparison *post hoc* test, n.s., not significant ($p > 0.05$). Box plots indicate means (black squares), medians (middle lines), 25th and 75th percentile ranges (boxes), and SD ranges (whiskers). Source data including the exact sample sizes and the p values are provided as a Source Data file.

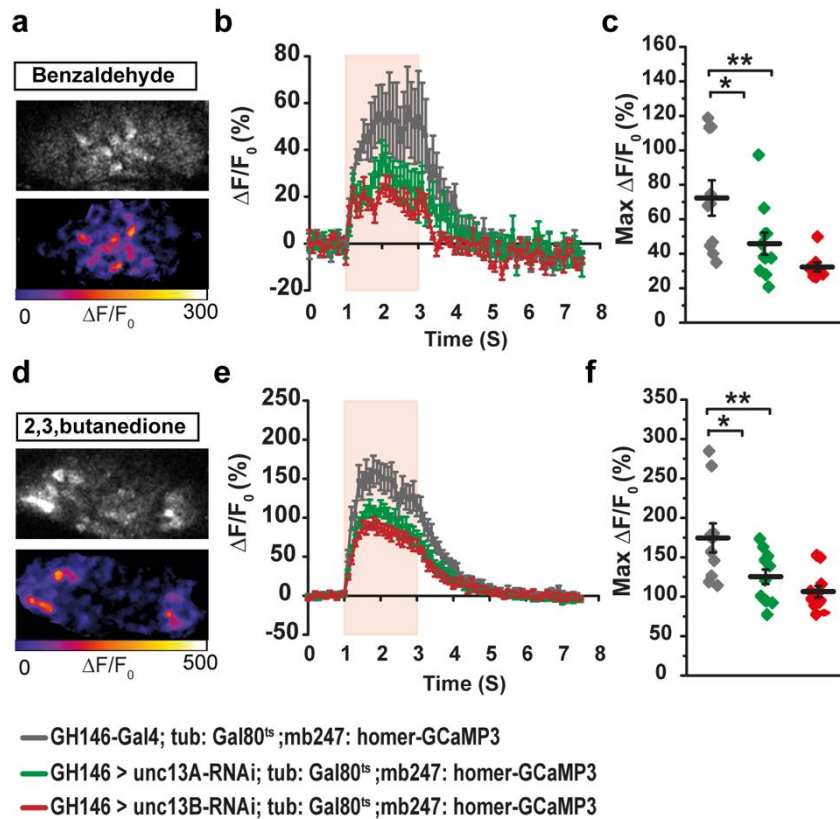


Supplementary Figure 9. Disruption of Unc13A dependent release by overexpressing *unc13A*-N-terminal fragment in ePNs. **a** Schematics of full length Unc13A (upper) and *unc13A*-N-term-GFP (lower) constructs indicating CaM, calmodulin; C1, C2B, C2C, and the MUN domain and the GFP tag. **b, c** Triple channel time gated STED (gSTED) images of GFP distribution (red) relative to BRP^{Nc82} (green) and Unc13B (blue) in calyx synapses in animals expressing UAS: *unc13A*-N-term-GFP under control of GH146-Gal4. Insets (**c**) show a planar BRP ring. GFP was found to be at 58.4 ± 1.2 nm (Mean \pm SEM) to the center of the BRP ring (n=4 brains, 244 synapses, experiment was performed once). Scale bars: **b** 200 nm, **c**. 100 nm White square indicates the magnified region. **d** Overexpression of *unc13A*-N-terminal fragment in ePNs under control of GH146-Gal4 leads to a significant reduction in performance index in response to both appetitive (2, 3-butanedione, n=20-22) and aversive (benzaldehyde, n=21-28) odors. All p-values were calculated via one-way ANOVA with the Bonferroni multiple comparison *post hoc* test (*p \leq 0.05). Box plots indicate means (black squares), medians (middle lines), 25th and 75th percentile ranges (boxes), and SD ranges (whiskers). Source data including the exact sample sizes and the p values are provided as a Source Data file.

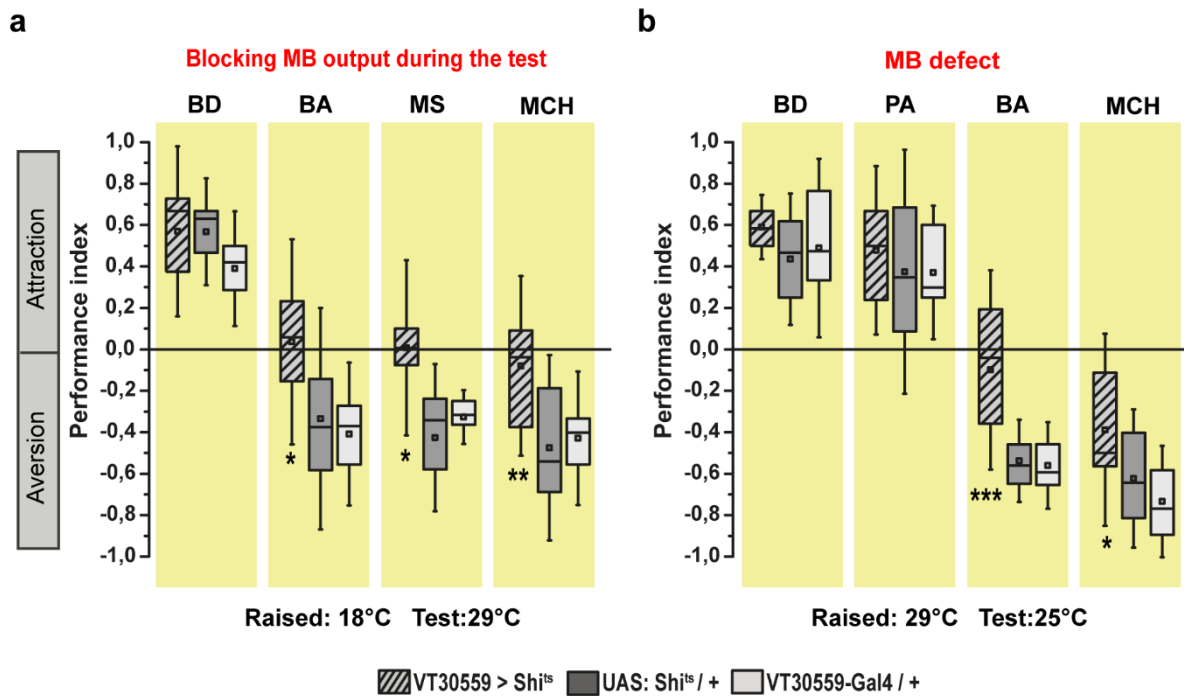


Supplementary Figure 10. Restriction of the *unc13A* or *unc13B* knockdown to adult stages using a tub: Gal80^{ts} approach **a** Confocal images from the calyx and the LH of animal expressing myr-RFP in ePNs under the control of GH146-Gal4 (GH146 > myr-RFP) immunostained against Unc13A (red), Unc13B (green) and RFP (blue). The yellow and white circles indicate the RFP⁺ and RFP⁻ boutons respectively. Scale bars: 5µm. **b** Confocal images from the calyx and the LH represent anti-BRP (green) and anti-Drep2 (red) immunostaining. Scale bars: 5 µm. **c** Expression level of Unc13A and Unc13B proteins in the RFP⁺ and RFP⁻ calycal boutons. The box plot shows a significant reduction of Unc13A in animals expressing *unc13A*-RNAi, myr-RFP (green plot) compared to the control group (gray plot) while no change was observed for Unc13B level. The level of Unc13B significantly reduced in animals expressing *unc13B*-RNAi, myr-RFP (red plot) compared to the control group (gray plot) while no change was observed for Unc13A level. In RFP⁻ calycal boutons, the level of Unc13A and Unc13B remains unchanged for all groups. **d** Expression level of Unc13A and Unc13B proteins in the RFP⁺ and RFP⁻ boutons of the LH. The box plot shows a significant reduction of Unc13A in animals expressing *unc13A*-RNAi, myr-RFP (green plot) compared to the control group (gray plot) while no change was observed for Unc13B levels. The levels of Unc13B significantly decreased in animals expressing *unc13B*-RNAi, myr-RFP (red plot) compared to the control group (gray plot) while no change was observed for Unc13A levels. In RFP⁻ boutons of the LH, the levels of Unc13A and Unc13B remains unchanged for all groups. **e, f** Quantification of BRP^{NC82} and Drep2 levels in the calyx (**e**) and the LH (**f**) boutons reveals no change

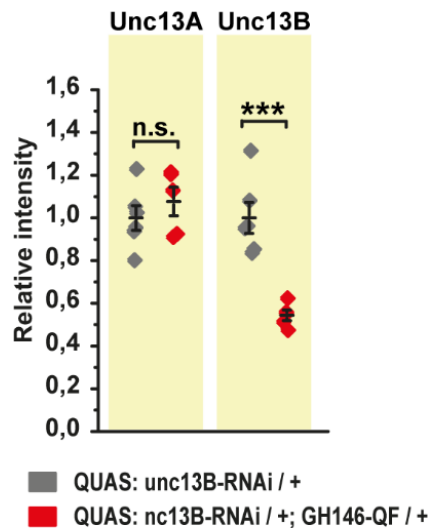
among different groups. Box plots indicate means (black squares), medians (middle lines), 25th and 75th percentile ranges (boxes), and 10–90% ranges (whiskers). $n=12-15$. All p-values were calculated via one-way ANOVA with the Bonferroni multiple comparison *post hoc* test (n.s., not significant ($p>0.05$), $*p\leq 0.05$, $**p\leq 0.01$, $***p\leq 0.001$). Source data including the exact sample sizes and the p values are provided as a Source Data file.



Supplementary Figure 11. Physiological deficit after *unc13A* or *unc13B* knockdown using the tub: Gal80^{ts} approach. **a, d** Representative false color-coded two-photon images of odor-induced fluorescence changes of GCaMP3 in MB calyx (mb247: homer-GCaMP3) at the dendritic terminals of Kenyon cells. For odor stimulation, benzaldehyde (**a**) and 2, 3-butanedione (**d**) were used. **b, e** Odor-induced fluorescence change ($\Delta F/F_0$) of homer-GCaMP3 in animals expressing UAS: *unc13A*-RNAi (green trace) or UAS: *unc13B*-RNAi (red trace) in ePNs under control of GH146-Gal4 in adult stage using tub:Gal80^{ts} was compared to the control group (GH146-Gal4/ tub: Gal80^{ts}; mb247: homer-Gcamp3^{+/+}, gray trace). **c, f** Maximum fluorescence changes of GCaMP3 upon odor stimulation, benzaldehyde (**c**) and 2, 3-butanedione (**f**) in animals with *unc13A* (green) or *unc13B* (red) knockdown compared to their genetic control (gray). For odor stimulation Benzaldehyde (n=8-12) and 2, 3-butanedione (n=10-12) were used. All p-values were calculated via one-way ANOVA with the Bonferroni multiple comparison *post hoc* test (*p \leq 0.05, **p \leq 0.01). All traces represent mean \pm SEM of $\Delta F/F_0$ % values. Error bars indicate SEM. Source data including the exact sample sizes and the p values are provided as a Source Data file.



Supplementary Figure 12. Mushroom bodies role in olfactory coding. **a** The output of MB neurons was blocked by expressing Shi^{ts} under control of VT30559-Gal4 driver line. Animals were kept at 18°C and tested at 29°C. Blocking the MB neurons at the time of test leads to a significant reduction in performance index of animals toward aversive odors (BA, n=9-12; MS, n=6 and MCH, n=8-14). No significant change was observed in VT30559> Shi^{ts} animals toward appetitive odor (BD, n=13-17). **b** Chronic blocking of the output of MB neurons by expressing Shi^{ts} under control of VT30559-Gal4 driver line and raising the animals at 29°C. The VT30559> Shi^{ts} animals with MB defect shows a significant reduction in performance index toward aversive odors (BA, n=12 and MCH, n=15-16) and no change toward appetitive odors (BD, n=13-17 and PA, n=10-13). BA: benzaldehyde, MS: methyl salicylate, MCH: 4-methylcyclohexanol, BD: 2, 3-butanedione, PA: propionic acid. All p-values were calculated via one-way ANOVA with the Bonferroni multiple comparison *post hoc* test (**p≤0.01, ***p≤0.001). Box plots indicate means (black squares), medians (middle lines), 25th and 75th percentile ranges (boxes), and SD ranges (whiskers). Source data including the exact sample sizes and the p values are provided as a Source Data file.



Supplementary Figure 13. Efficient Knockdown of *unc13B* in ePNs using QUAS/QF system. Expression level of Unc13A and Unc13B proteins in calycaal boutons in animals expressing QUAS: *unc13B*-RNAi under control of GH146-QF, compared to the control group. The values show a significant reduction of Unc13B in *unc13B*-knockdown group (red plot) compared to the control group (gray plot) while no change was observed for Unc13A level. P-values were calculated via two-sample t-test. (n.s., not significant ($p > 0.05$), *** $p \leq 0.001$, $n = 5-6$). Values represent mean \pm SEM. Source data including the exact sample sizes and the p values are provided as a Source Data file.

Primer name	Primer sequence
UAS- gypsy F1	CGACAAGCCGAATTGATCCACTAGAAAGGCCTAATTCGGTACACTAGT
UAS- gypsy R1	CACGTGACTCGAGAAAGAGAGAGAGAAAGCTGGTACTACTAGTGTTGTTG
UAS- gypsy F1	ACACTAGTAGTACCAGCTTTCTCTCTCTTTCTCGAGTCACGTG
UAS- gypsy R2	AGCGTAGCGGATCCGTAAGCTTCGGCTATCGAGTCACTGAGTCCCAACGTGAAAGG

Supplementary Table 1. Sequences of primers used in this study.